# Synthetic Topological Nodal Phase in Bilayer Resonant Gratings

Ki Young Lee,[1,*] Kwang Wook Yoo,[1,*] Sangmo Cheon,[1] Won-Jae Joo,[2] Jae Woong Yoon,[1,†] and Seok Ho Song[1,‡]

[1]*Department of Physics, Hanyang University, Seoul 133-791, Korea*

[2]*Samsung Advanced Institute of Technology, Samsung Electronics, Suwon 16678, Korea*

(Received 31 August 2021; accepted 3 January 2022; published 2 February 2022)

The notion of synthetic dimensions in artificial photonic systems has received considerable attention as it provides novel methods for exploring hypothetical topological phenomena as well as potential device applications. Here, we present nanophotonic manifestation of a two-dimensional topological nodal phase in bilayer resonant grating structures. Using the mathematical analogy between a topological semimetal and vertically asymmetric photonic lattices, we show that the interlayer shift simulates an extra momentum dimension for creating a two-dimensional topological nodal phase. We present a theoretical model and rigorous numerical analyses showing the two nodal points that produce a complex gapless band structure and localized edge states in the topologically nontrivial region. Therefore, our results provide a practical scheme for producing high-dimensional topological effects in simple low-dimensional photonic structures.

DOI: 10.1103/PhysRevLett.128.053002

Along with the growing interest in the topological insulators [1,2], the search for diverse topological phases of matter has been emerged as a new frontier in the field of quantum materials. A remarkable discovery is the topological nodal phases [3] as found in the Dirac or Weyl semimetals [4,5]. They show topologically nontrivial regions in their gapless band structures possessing an exotic surface state on the Fermi arcs. In this regard, the novel topological notions are found in various wave systems such as electronic [6], atomic [7], phononic [8,9], and photonic [10–12] lattices. Importantly, these systems show additional phenomena associated with non-Hermitian [13,14] and high dimensional topological phases [15,16]. Although such phenomena are of fundamental interest and also hold some potential for practical applications, they often imply hypothetical potential distributions that have no counterparts in the existing condensed matter systems.

Within this context, the concept of synthetic dimensions [17,18] represents the nonspatial degrees of freedom which are parametric replacements of actual spatial dimensions of a system Hamiltonian, offering new schemes for experimentally realizing high-dimension topological phenomena in simple low-dimensional systems. For instance, three-dimensional (3D) Weyl points have been reported in 1D photonic lattices [19], sonic crystals [20,21], and 2D ring-resonator systems [22] taking geometrical shape factors or on-site frequency components as synthetic-dimension parameters. Thus, the use of synthetic dimensions provides an efficient means to implement fundamental topological phenomena as well as additional functionalities enabling one-way frequency conversion [22], topological rainbow trapping [23], and vortex beam generation [19,24].

In this Letter, we propose bilayer resonant gratings as a new platform for constructing photonic topological nodal phases in a synthetic momentum dimension. We show that the interlayer shift simulates a synthetic wave vector controlling the complex Berry phase [25] of non-Hermitian photonic band structures. Previously, the interlayer shift has been treated as a Hermitian band-tuning parameter for the flat or Dirac-crossing dispersion relations in multilayer photonic systems such as twisted bilayer photonic crystals [26,27], photonic fishbone lattice [28], moiré metasurfaces [29–31].

Here, we take a further step toward the non-Hermitian topological physics, where the characteristic band tuning effects are understood as natural consequences of the topological phase transition while the non-Hermiticity suggests intriguing opportunities for novel probing and resonance control schemes. We provide complex band structures of guided-mode-resonance (GMR) states over a 2D synthetic-momentum space, an analytic theory based on the photonic analogy of topological semimetals, and consistent rigorous numerical calculation results. Therein, the topological phase transition emerges with an edge-state dispersion connecting two Dirac points. Intriguingly, these characteristic features clearly appear in the far-field intensity distributions as resonance spectra potentially useful for a variety of nanophotonic applications in practice.

We consider a bilayer configuration consisting of two identical 1D dielectric subwavelength gratings as schematically illustrated in Fig. 1. The structure has total thickness $d$, fill factor $F$, period $a$, and grating bars with refractive index $n_1$ covered by a low index medium denoted by its refractive index $n_2$. We introduce the degree $S$ of lateral interlayer shift between the two layers, which adjusts

 

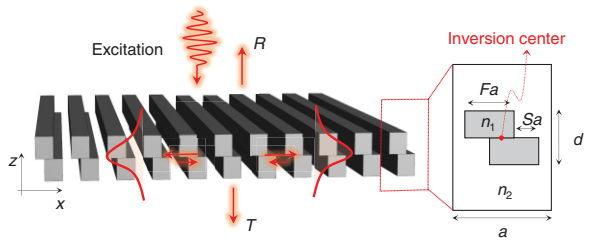


FIG. 1. Schematic of an asymmetric bilayer grating for synthetic topological nodal phase. The structure consists of two identical thin-film photonic lattices with fill factor $F$, refractive index $n_1$, period $a$, and total thickness $d$. Degree of interlayer shift between two layers is denoted by $S$.

the interlayer interaction with a normalized value from 0 to 1. The unit cell configuration with the lateral shift maintains the inversion symmetry of the structure as shown in the right inset of Fig. 1. We assume light incidence in the zero-order regime below the Rayleigh frequency and analyze optical responses near the second-order Bragg-reflection condition for $TE_0$ guided modes of the entire slab [32,33].

The complex GMR band structures in this bilayer-grating structure are described by a non-Hermitian eigenvalue problem $\mathbf{H}_{\mathrm{GMR}}|\psi\rangle = E|\psi\rangle$, where eigenvalue $E$ is complex due to leakage radiation of the GMR states toward the radiation continuum in the background medium. Considering $S$ as an additional degree of freedom in the interlayer interaction, the Hamiltonian $\mathbf{H}_{\mathrm{GMR}}$ is written by the following form.

$$\mathbf{H}_{\mathrm{GMR}} = (\kappa + i\gamma)\cos 2\pi S\boldsymbol{\sigma}_x - k_x v_g \boldsymbol{\sigma}_y. \tag{1}$$

Here, $\kappa$ represents total coupling rate between the counterpropagating guided modes, and $\gamma$ denotes the leakage-radiation rate of the guided modes. $\kappa$ and $\gamma$ are assumed to be positive and real valued in our configuration. $k_x$ is the transverse Bloch wave vector, $v_g$ denotes the group speed of the guided mode, and $\boldsymbol{\sigma}_j$ represents the Pauli matrices. See Supplemental Material for the mathematical details [34–37].

We note that $\mathbf{H}_{\mathrm{GMR}}$ in Eq. (1) is in an exact mathematical analogy to the 2D topological nodal phase Hamiltonian for a chiral-symmetric semimetal configuration under the low-energy continuum approximation [38]. The full band bulk Hamiltonian $\mathbf{H}_{\mathrm{TNP}}$ in the parametric parallelism with $\mathbf{H}_{\mathrm{GMR}}$ can be written as

$$\mathbf{H}_{\mathrm{TNP}} = [v_g(1-\cos p_x) - (\kappa + i\gamma)\cos p_S]\boldsymbol{\sigma}_x + v_g \sin p_x \boldsymbol{\sigma}_y, \tag{2}$$

where spatial wave vector $p_x = k_x + \pi$ and synthetic wave vector $p_S = 2\pi S$ constitute a synthetic 2D momentum space—one momentum dimension with $k_x$ and another synthetic dimension with $S$. In the presence of the leakage radiation loss ($\gamma > 0$),$\mathbf{H}_{\mathrm{TNP}}$ results in a complex-valued band structure in the synthetic $p_x$-$p_S$ domain as shown in Fig. 2(a). In particular, the real and imaginary band structures include the two nodal points at $p_x = 1.0$, and $p_S = 0.5\pi$ or $1.5\pi$ ($S = 0.25$ or 0.75). These nodal points are the 1D Dirac points (DPs) along $p_x$ since the non-Hermiticity disappears by formation of the flat imaginary bands as denoted by white dashed lines in Fig. 2(a).

The complex band structures in Fig. 2(a) also reveal the $p_S$-dependent band topology in which the skin color indicates the relative even-eigenvector strength $|\langle \mathrm{even}|\psi\rangle, |\mathrm{where}|\mathrm{even}\rangle = 2^{-1/2}[1\ 1]^T$. The band flip by the eigenvector exchange occurs between the two DPs ($0.25 < S < 0.75$), and this region represents the bilayer photonic lattice in the topologically nontrivial phase.

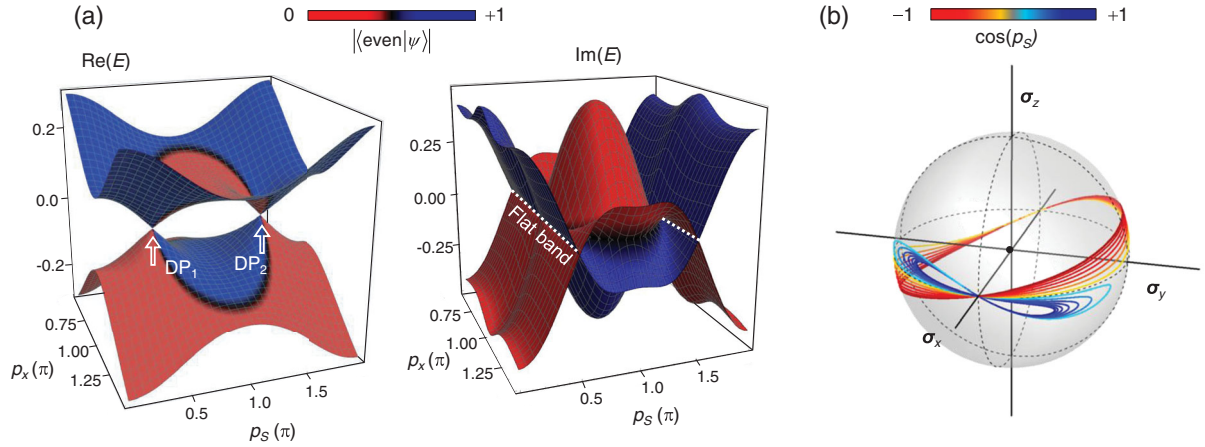


FIG. 2. Complex bulk band features of a topological nodal phase Hamiltonian. (a) Real (left) and imaginary (right) energy band structures in 2D synthetic space $(p_x, p_S)$ for $\mathbf{H}_{\mathrm{TNP}}$ in Eq. (2). Parameters are $v_g = 1.5$, $\kappa = 1$, and $\gamma = 0.5$. Two Dirac points (DPs) are denoted by white arrows in the real band. White dashed lines in the imaginary band on the right indicate flat bands along the $p_x$ axis at $p_S = 0.5\pi$ and $1.5\pi$. Skin color indicates relative even-mode strength for corresponding eigenvectors. (b) Bloch sphere representation **b** of the lower-band eigenvector for geometric picture of the quantized complex Berry phase. Line color indicates $\cos(p_S)$ value.

This $S$-dependent non-Hermitian topological phase is also identified by the quantized complex Berry phase which is known as a topological invariant for chiral-symmetric non-Hermitian Hamiltonians such that $\boldsymbol{\sigma}_z\mathbf{H}\boldsymbol{\sigma}_z = -\mathbf{H}$. The definition of the complex Berry phase is $Q_\pm = i\oint\langle\xi_\pm|\partial_{kx}|\psi_\pm\rangle dk_x$ where the subscript $\pm$ denotes upper $(+)$ or lower $(-)$ band, respectively. The left $|\xi\rangle$ and right $|\psi\rangle$ eigenvectors of $\mathbf{H}$ are related by the conjugated pseudo-Hermiticity such that $|\xi\rangle = \sigma_x|\psi\rangle^*$. Under these constraints, the complex Berry phase is quantized at 0 and $\pi$ [25].

In order to directly visualize the geometric picture of the complex Berry phase transition with the change in $S$, we plot the lower-eigenvector path of the Bloch vector $\mathbf{b} = \langle\psi_-|\boldsymbol{\sigma}|\psi_-\rangle$ within the first Brillouin zone of $k_x$ in Fig. 2(b). The quantized complex Berry phase is $\pi$ when the $\mathbf{b}$-path curve encircles around $\boldsymbol{\sigma}_z$ axis, while it takes 0 otherwise. The line color for the $\mathbf{b}$-path curve indicates the synthetic dimension value $\cos(p_S)$ and clearly reveals the complex Berry phase $Q_-$ quantized at 0 and $\pi$. Therefore, the bulk Hamiltonian of the bilayer photonic lattice implies the nontrivial topological phase in the region between the two DPs ($0.25 < S < 0.75$), indicating the manifestation of a gapless topological GMR state for a finite structure with an open boundary.

We provide a specific numerical example for demonstrating the manifestation of the topological nodal phase in the proposed synthetic dimension and associated photonic states. We design a bilayer structure consisting of two identical Si-grating layers ($n_1 = 3.48$) covered by a $Si_3N_4$ background ($n_2 = 2.45$). We assume an interface between the bilayer grating and perfect electric conductor (PEC) as an optical hard wall for accommodating the edge states in the topologically nontrivial region in the synthetic dimension. We include 50 periods with the PEC boundary condition at both sides in the numerical eigenvalue calculations using the finite-element method.

Figure 3(a) shows the projected complex dispersion relations of the bilayer Si grating in the normalized frequency $a/\lambda$ and synthetic parameter $S$ domain. We assume $d = 200$ nm, fill factor $F = 0.8$, and $a = 480$ nm in this calculation. The calculation result shows essential characteristics of the complex band structures predicted by the bulk Hamiltonian of the topological nodal phase in Eq. (2). It includes the simultaneous gap closing of the real and imaginary bands at $S = 0.25$ and 0.75. The gapless dispersion indicated by the dark-red curves shows the emergence of the topological edge states connecting the two DPs in the topologically nontrivial region of $S$. Note that we distinguish the topological edge and trivial Bloch state bands with color-coded edge localization factor $N^{-1}\int_0^a\int_{-d/2}^{d/2}|E_y(x,y)|^2dx\,dz$ indicating the normalized electric-field energy content in the first period from the PEC-lattice boundary. For this topological edge state, we present the field distribution $|E_y(x,z)|$ on the $x$-$z$ plane at the strongest localization for $S = 0.5$ in Fig. 3(b). It shows typical edge-localization characteristics.

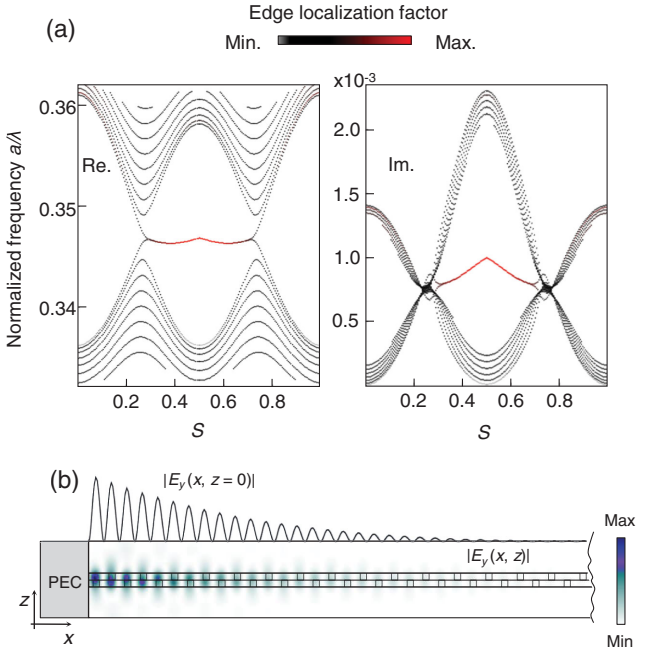


FIG. 3. Open boundary complex energy spectra and gapless topological edge states in bilayer gratings. (a) Projected real (left) and imaginary (right) dispersion relations in the normalized frequency and synthetic parameter space. Line color indicates edge localization factor—edge states are in red and bulk Bloch states are in black. (b) Spatial distribution of electric field norm $|E_y(x,z)|$ for the topological edge state at $S = 0.5$.

We compare the numerical results with the model Hamiltonian in Eq. (1) as provided in Sec. 2 and Fig. S1 of Supplemental Material [34–37]. Although we find the notable difference in the imaginary band splitting for the topologically nontrivial phase region due to high-order diffraction from the sharp index discontinuity at the edges of the grating bars, the two results show a quantitative agreement for the emergence of the two nodal points in the complex band structures at $S = 0.25$ and 0.75, indicating that the discrepancy does not change the essential topological physics.

We further investigate the manifestation of the synthetic topological nodal phase in the resonant reflection spectrum. In this analysis, we assume a photonic junction consisting of the two bilayer gratings with different $S$—one on the left takes an arbitrary $S$ value while the other on the right takes a fixed lateral shift at $S = 0$, as shown in Fig. 4(a). In Fig. 4(b), we show the calculated reflectance spectrum under the normal incidence of TE-polarized plane wave in $(a/\lambda, S)$ domain. We apply the periodic boundary condition in the $x$ axis such that the supercell unit includes 50 periods. The result shows the resonant peaks in response to the excitation of the leaky photonic modes at $k_x = 0$. In particular, the resonance feature at $a/\lambda \approx 0.347$ for $0.25 < S < 0.75$ represents the photonic Jackiw-Rebbi-state

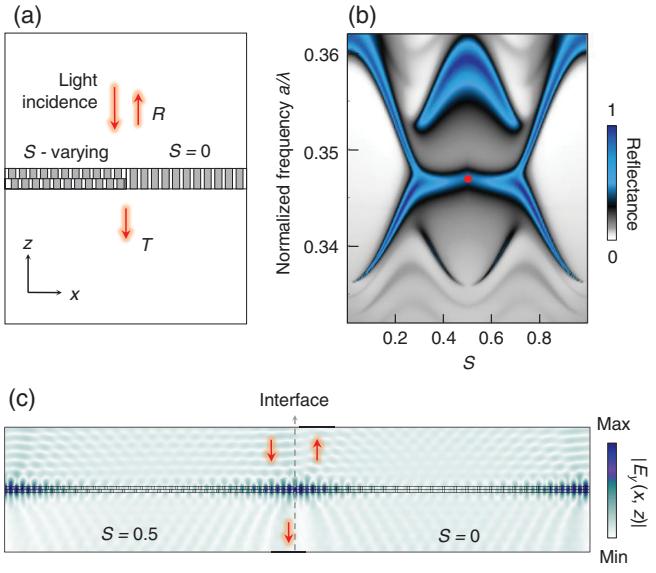


FIG. 4. Resonant spectral responses of topological nodal phase under plane wave incidence. (a) Schematic of photonic junction consisting of two bilayer gratings, one on the left with variable $S$ and the other on the right with fixed $S = 0$. (b) Resonant reflection spectra depending on $S$. (c) Spatial distribution of electric field norm for the Jakiw-Rebbi-state resonance at $S = 0.5$ and $a/\lambda = 0.347$ as denoted by red dot in Fig. 4(b).

resonance [37] as confirmed by the associated field distributions in Fig. 4(c). The spectral loci of these Jackiw-Rebbi-state resonances follow the edge-state dispersion in Fig. 3(a) as they both are zero-energy states emerging at the midpoint of the frequency band gap.

In conclusion, we propose a 1D bilayer subwavelength grating structure for the 2D topological nodal phases in an efficiently controllable synthetic dimension. The degree of the interlayer shift provides an additional synthetic-momentum dimension required for DP formation in a simple 1D lattice structure. We show that the proposed synthetic dimension supports fundamental physics related to the non-Hermitian 2D topological nodal phases involving the characteristic complex band structures, quantized complex Berry phase, topological localization, and their interaction with the radiation continuum. The numerical results for open boundary dispersions show the complex gapless dispersion of the topological edge states which connect the two DPs in the topologically nontrivial region of the synthetic dimension.

The proposed synthetic-dimension approach uses the band dynamics enabled by constructive or destructive interference between the counterpropagating GMR states, which is clearly distinguished by existing parametric modulation methods that directly manipulate spatial Fourier coefficients of the unit-cell configuration [19–22]. This may provide an efficient scheme for exploring high-dimensional topological nodal phases with the current state-of-the-art nanofabrication technology [39]. These nonspatial degrees of freedom in 2D bilayer photonic configurations such as layer-mixed topological heterojunctions [40] and glide symmetric structures [41] in terms of synthetic dimensions suggest possible scenarios for 3D topological phenomena including the Weyl physics.

In addition, we note that control of the interlayer shift enables formation of the flat-imaginary band as well as generation of quasibound states in the continuum [42] by changing the real and imaginary band structures simultaneously. This property also suggests that one can efficiently control radiative loss of a resonant state by a simple topological parametric change which is not considered in the conventional chiral and moiré gratings [26–31]. Therefore, associated theoretical and experimental study may create novel methods for topological $Q$-factor engineering in thin-film nanophotonics applications [43–45].

The leakage-radiation-induced non-Hermiticity in our specific case pertains to the conjugated pseudo-Hermiticity due to the unbroken chiral symmetry. Thereby, the Hermitian-continuable topological states manifest, not purely non-Hermitian effects [46]. Nevertheless, the out-of-plane leakage radiation provides intriguing opportunities to probe internal topological properties [47] and to develop topological photonic engineering of far-field optical signals. Toward this end, we introduce here the manifestation of a synthetic topological nodal phase in the out-of-plane leakage radiation domain as characteristic resonance spectra in the optical far field. In further consideration, it is of great interest to simultaneously include the leakage radiation and intrinsic gain-loss configurations. In such systems, one may expect novel far-field optical effects produced by purely non-Hermitian, non-chiral-symmetric topological phenomena such as parity-time-symmetric exceptional hypersurfaces [48] and non-Hermitian skin effects [49,50].

This research was supported in part by the Basic Science Research Program (NRF-2018R1A2B3002539), the Leader Researcher Program (NRF-2019R1A3B2068083), and the research fund of Hanyang University (HY-202000000000513). K. Y. L and S. H. S. acknowledge additional support from Global Ph.D. Fellowship Program (NRF-2017H1A2A1042111) and from Samsung Electronics, respectively.

*These authors contributed equally to this work.
†To whom correspondence should be addressed.
yoonjw@hanyang.ac.kr
‡To whom correspondence should be addressed.
shsong@hanyang.ac.kr

[1] M. Z. Hasan and C. L. Kane, Colloquium: Topological insulators, Rev. Mod. Phys. **82**, 3045 (2010).
[2] X. L. Qi and S. C. Zhang, Topological insulators and superconductors, Rev. Mod. Phys. **83**, 1057 (2011).
[3] A. A. Burkov, M. D. Hook, and L. Balents, Topological nodal semimetals, Phys. Rev. B **84**, 235126 (2011).

[4] Z. K. Liu, B. Zhou, Y. Zhang, Z. J. Wang, H. M. Weng, D. Prabhakaran, S. Mo, Z. X. Shen, Z. Fang, X. Dai, Z. Hussain, and Y. L. Chen, Topological dirac semimetal, $Na_3Bi$, Science **343**, 864 (2014).

[5] S. Y. Xu *et al.*, Discovery of a Weyl fermion semimetal and topological fermi arcs, Science **349**, 613 (2015).

[6] S. Cheon, T. H. Kim, S. H. Lee, and H. W. Yeom, Chiral solitons in a coupled double peierls chain, Science **350**, 182 (2015).

[7] B. K. Stuhl, L. M. Aycock, D. Genkina, and I. B. Spielman, Visualizing edge states with an atomic Bose gas in the quantum Hall regime, Science **349**, 1514 (2015).

[8] C. L. Kane and T. C. Lubensky, Topological boundary modes in isostatic lattices, Nat. Phys. **10**, 39 (2014).

[9] M. Xiao, G. Ma, Z. Yang, P. Sheng, Z. Q. Zhang, and C. T. Chan, Geometric phase and band inversion in periodic acoustic systems, Nat. Phys. **11**, 240 (2015).

[10] L. Lu, L. Fu, J. D. Joannopoulos, and M. Soljacic, Weyl points and line nodes in gyroid photonic crystals, Nat. Photonics **7**, 294 (2013).

[11] L. Lu, Z. Wang, D. Ye, L. Ran, L. Fu, J. D. Joannopoulos, and M. Soljačić, Experimental observation of Weyl points, Science **349**, 622 (2015).

[12] T. Ozawa, H. M. Price, A. Amo, N. Goldman, M. Hafezi, L. Lu, M. C. Rechtsman, D. Schuster, J. Simon, O. Zilberberg, and I. Carusotto, Topological photonics, Rev. Mod. Phys. **91**, 015006 (2019).

[13] E. J. Bergholtz, J. C. Budich, and F. K. Kunst, Exceptional topology of non-Hermitian systems, Rev. Mod. Phys. **93**, 015005 (2021).

[14] A. Cerjan, S. Huang, M. Wang, K. P. Chen, Y. Chong, and M. C. Rechtsman, Experimental realization of a Weyl exceptional ring, Nat. Photonics **13**, 623 (2019).

[15] A. Dutt, M. Minkov, I. A. D. Williamson, and S. Fan, Higher-order topological insulators in synthetic dimensions, Light Sci. Appl. **9**, 131 (2020).

[16] O. Zilberberg, S. Huang, J. Guglielmon, M. Wang, K. P. Chen, Y. E. Kraus, and M. C. Rechtsman, Photonic topological boundary pumping as a probe of 4D quantum Hall physics, Nature (London) **553**, 59 (2018).

[17] L. Yuan, Q. Lin, M. Xiao, and S. Fan, Synthetic dimension in photonics, Optica **5**, 1396 (2018).

[18] E. Lustig and M. Segev, Topological photonics in synthetic dimensions, Adv. Opt. Photonics **13**, 426 (2021).

[19] Q. Wang, M. Xiao, H. Liu, S. Zhu, and C. T. Chan, Optical Interface States Protected by Synthetic Weyl Points, Phys. Rev. X **7**, 031032 (2017).

[20] X. Fan, C. Qiu, Y. Shen, H. He, M. Xiao, M. Ke, and Z. Liu, Probing Weyl Physics with One-Dimensional Sonic Crystals, Phys. Rev. Lett. **122**, 136802 (2019).

[21] Z. Wang, Z. Wang, H. Li, J. Luo, X. Wang, Z. Liu, and H. Yang, Weyl points and nodal lines in acoustic synthetic parameter space, Appl. Phys. Express **14**, 077002 (2021).

[22] Q. Lin, M. Xiao, L. Yuan, and S. Fan, Photonic Weyl point in a two-dimensional resonator lattice with a synthetic frequency dimension, Nat. Commun. **7**, 13731 (2016).

[23] C. Lu, C. Wang, M. Xiao, Z. Q. Zhang, and C. T. Chan, Topological Rainbow Concentrator Based on Synthetic Dimension, Phys. Rev. Lett. **126**, 113902 (2021).

[24] H. Cheng, W. Gao, Y. Bi, W. Liu, Z. Li, Q. Guo, Y. Yang, O. You, J. Feng, H. Sun, J. Tian, S. Chen, and S. Zhang, Vortical Reflection and Spiraling Fermi Arcs with Weyl Metamaterials, Phys. Rev. Lett. **125**, 093904 (2020).

[25] S. Lieu, Topological phases in the non-Hermitian Su-Schrieffer-Heeger model, Phys. Rev. B **97**, 0045106 (2018).

[26] K. Dong, T. Zhang, J. Li, Q. Wang, F. Yang, Y. Rho, D. Wang, C. P. Grigoropoulos, J. Wu, and J. Yao, Flat Bands in Magic-Angle Bilayer Photonic Crystals at Small Twists, Phys. Rev. Lett. **126**, 223601 (2021).

[27] B. Lou, N. Zhao, M. Minkov, C. Guo, M. Orenstein, and S. Fan, Theory for Twisted Bilayer Photonic Crystal Slabs, Phys. Rev. Lett. **126**, 136101 (2021).

[28] H. S. Nguyen, F. Dubois, T. Deschamps, S. Cueff, A. Pardon, J. L. Leclercq, C. Seassal, X. Letartre, and P. Viktorovitch, Symmetry Breaking in Photonic Crystals: On-Demand Dispersion from Flatband to Dirac Cones, Phys. Rev. Lett. **120**, 066102 (2018).

[29] Z. Wu and Y. Zheng, Moiré chiral metamaterials, Adv. Opt. Mater. **5**, 1700034 (2017).

[30] P. Wang, Y. Zheng, X. Chen, C. Huang, Y. V. Kartashov, L. Torner, V. V. Konotop, and F. Ye, Localization and delocalization of light in photonic moiré lattices, Nature (London) **577**, 42 (2020).

[31] S. S. Sunku, G. X. Ni, B. Y. Jiang, H. Yoo, A. Sternbach, A. S. McLeod, T. Stauber, L. Xiong, T. Taniguchi, K. Watanabe, P. Kim, M. M. Fogler, and D. N. Basov, Photonic crystals for nano-light in moiré graphene superlattices, Science **362**, 1153 (2018).

[32] D. Rosenblatt, A. Sharon, and A. A. Friesem, Resonant grating waveguide structures, IEEE J. Quantum Electron. **33**, 2038 (1997).

[33] S. S. Wang and R. Magnusson, Theory and applications of guided-mode resonance filters, Appl. Opt. **32**, 2606 (1993).

[34] See Supplemental Material at http://link.aps.org/supplemental/10.1103/PhysRevLett.128.053002 for mathematical details, which includes Refs. [35–37].

[35] Y. Ding and R. Magnusson, Band gaps and leaky-wave effects in resonant photonic-crystal waveguides, Opt. Express **15**, 680 (2007).

[36] K. Y. Lee, K. W. Yoo, Y. Choi, G. Kim, S. Cheon, J. W. Yoon, and S. H. Song, Topological guided-mode resonances at non-Hermitian nanophotonic interfaces, Nanophotonics **10**, 1853 (2021).

[37] S. G. Lee and R. Magnusson. Band flips and bound-state transitions in leaky-mode photonic lattices, Phys. Rev. B **99**, 045304 (2019).

[38] C. K. Chiu and A. P. Schnyder, Classification of reflection-symmetry-protected topological semimetals and nodal superconductors, Phys. Rev. B **90**, 205136 (2014).

[39] Y. Horie, A. Arbabi, S. Han, and A. Faraon, High resolution on-chip optical filter array based on double subwavelength grating reflectors, Opt. Express **23**, 29848 (2015).

[40] X. D. Chen, X. T. He, and J. W. Dong, All-dielectric layered photonic topological insulators, Laser Photonics Rev. **13**, 1900091 (2019).

[41] Y. Wang, J. Wei You, Z. Lan, and N. C. Panoiu, Topological valley plasmon transport in bilayer graphene metasurfaces for sensing applications, Opt. Lett. **45**, 3151 (2020).

[42] C. W. Hsu, B. Zhen, A. D. Stone, J. D. Joannopoulos, and M. Soljacic, Bound states in the continuum, Nat. Rev. Mater. **1**, 16048 (2016).

[43] S. G. Lee, S. H. Kim, and C. S. Kee, Metasurfaces with Bound States in the Continuum Enabled by Eliminating First Fourier Harmonic Component in Lattice Parameters, Phys. Rev. Lett. **126**, 013601 (2021).

[44] A. I. Kuznetsov, A. E. Miroshnichenko, M. L. Brongersma, Y. S. Kivshar, and B. Luk'yanchuk, Optically resonant dielectric nanostructures, Science **354**, aag2472 (2016).

[45] W. J. Joo, J. Kyoung, M. Esfandyarpour, S. H. Lee, H. Koo, S. Song, Y. N. Kwon, S. H Song, J. C. Bae, A. Jo, M. J. Kwon, S. H. Han, S. H. Kim, S. Hwang, and M. L. Brongersma, Metasurface-driven OLED displays beyond 10,000 pixels per inch, Science **370**, 459 (2020).

[46] D. Leykam, K. Y. Bliokh, C. Huang, Y. D. Chong, and F. Nori, Edge Modes, Degeneracies, and Topological Numbers in Non-Hermitian Systems, Phys. Rev. Lett. **118**, 040401 (2017).

[47] D. Leykam and D. A. Smirnova, Probing bulk topological invariants using leaky photonic lattices, Nat. Phys. **17**, 632 (2021).

[48] Q. Wang, K. Ding, H. Liu, S. Zhu, and C. T. Chan, Exceptional cones in 4D parameter space, Opt. Express **28**, 1758 (2020).

[49] V. M. Martinez Alvarez, J. E. Barrios Vargas, and L. E. F. Foa Torres, Non-Hermitian robust edge states in one dimension: Anomalous localization and eigenspace condensation at exceptional points, Phys. Rev. B **97**, 121401(R) (2018).

[50] S. Yao and Z. Wang, Edge States and Topological Invariants of Non-Hermitian Systems, Phys. Rev. Lett. **121**, 086803 (2018).